Generalized Anomeric Effect in $CH_{4-n}Cl_nS$. Energetic and NBO Analyses

Hossein Roohi* and Sayed Mostefa Habibi

Department of Chemistry, Faculty of Science, University of Sistan and Baluchestan, P. O. Box 98135-674, Zahedan, Iran

Received October 19, 2006; E-mail: hroohi@hamoon.usb.ac.ir

The conformational preference for *gauche* structures over anti ones in the simple model molecules $CH_{4-n}Cl_nS$ (where $n = 1$ and 2) was examined in detail by means of Natural Bond Orbital (NBO) analysis. We also compared the origin of the anomeric effect in CH_2ClSH and CH_2FSH. The energetic preference at MP2/6-311+G(d,p) level was slightly greater in CH_2ClSH than in $CHCl_2SH$. NBO analysis at the HF/6-311+G(d,p)//MP2/6-311+G(d,p) level indicates that the conformational preference for *gauche* conformers over *anti* ones is the result of a wide variety of orbital interactions. However, the interaction between the lp(S) and σ^*(C–Cl) is the most important factor for stabilizing the *gauche* conformers. In all compounds studied here, the effect of electrostatic and steric contributions involved in the Lewis term on stability of *gauche* conformers was less important than the charge delocalization.

The hyperconjugative interactions are ubiquitous in organic chemistry and lead to significant changes in geometry,[1,2] electron density distribution, MO energy, IR spectra, bond strengths,[3,4] and NMR spectra.[5,6] The generalized anomeric effect (GAE) is recognized in an R–X–B–Y moiety as the strong preference for the *gauche* orientation of the R–X bond with respect to the B–Y one.[7–10] A large number of experimental and theoretical studies have been carried out in order to provide an explanation for anomeric effect.[11–35]

We have recently investigated the origin of the anomeric effect in fluoromethanol[36] and fluoromethanethiol.[37] In a continuation of our study on the AE and rotational barrier, we attempted to analyze origin of this effect in $CH_{4-n}Cl_nS$ (where $n = 1$ and 2) (Scheme 1). In addition, the variation of the AE going from CH_2FSH to CH_2ClSH was examined.

Results and Discussion

Energetics and Geometries. Table 1 presents the following relative thermodynamic properties of studied molecules, that is, change of enthalpy (ΔH), change of Gibbs free energy (ΔG), and change of entropy (ΔS), calculated at the HF/6-311+G(d,p), B3LYP/6-311+G(d,p), and MP2/6-311+G(d,p)

levels and dipole moments (μ) at MP2/6-311+G(d,p) level. Optimized structural parameters obtained at the MP2/6-311+G(d,p) level are given in Table 2.

CH_2ClSH (1a–1c). Figures 1a and 1b show the C–S rotational potential for **1a** compound at the MP2/6-311G(d,p) level of theory. The Gibbs free energy of activation ($\Delta G^{\#}$) and enthalpy of activation ($\Delta H^{\#}$) for the internal rotation about the C–S bond in the **1a** and **1c** compounds calculated at the MP2/6-311+G(d,p) level of theory are listed at the top of potential scan curves in Figs. 1a and 1c, respectively.
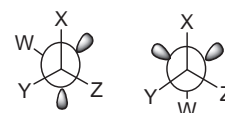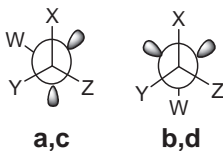

a,c   **b,d**

1a, 1b: X = Cl, Y = Z = W = H
1c: X = Y = Z = H, W = Cl
2a, 2b: X = Y = Cl, Z = W = H
2c, 2d: X = W = Cl, Y = Z = H

Scheme 1.

Table 1. Calculated Conformational Energy (kJ mol⁻¹) and Entropy (J mol⁻¹ K⁻¹) at the B3LYP/6-311+G(d,p), HF/6-311+G(d,p), and MP2/6-311+G(d,p) Levels and Dipole Moment (Debye) at MP2/6-311+G(d,p) Level

Compd.	B3LYP/6-311+G(d,p)			HF/6-311+G(d,p)			MP2/6-311+G(d,p)			
	ΔH[a]	ΔG[b]	ΔS	ΔH[a]	ΔG[b]	ΔS	ΔH[a]	ΔG[b]	ΔS	μ
1a	0.0	0.0	0.0	0.0	0.0	0.0	0.0	0.0	0.0	1.75
1b	12.7	9.3	11.5	9.3	7.8	4.1	11.4	6.1	17.8	2.84
1c	18.5	17.2	4.3	26.5	25.5	3.3	42.0	40.8	4.0	2.51
2a	0.0	0.0	0.0	0.0	0.0	0.0	0.0	0.0	0.0	0.81
2b	3.8	3.6	0.6	2.5	2.5	−0.1	3.5	3.3	0.5	2.05
2c	9.3	7.7	5.4	14.2	12.8	4.6	39.9	38.4	5.0	2.37
2d	28.1	25.4	9.1	19.4	15.3	7.3	46.9	44.18	10.8	1.18

a) Sum of electronic energy and thermal enthalpy differences. b) Sum of electronic energy and thermal free energy differences.

Table 2.   Optimized Geometrical Parameters of Molecules **1a–1d** at MP2/6-311+G(d,p) Level[a]

	1a	**1b**	**1c**	**2a**	**2b**	**2c**	**2d**
C–X	1.785 (1.775)[b]	1.772	1.091	1.780	1.770	1.779	1.770
C–Y	1.088	1.088	1.091	1.780	1.779	1.089	1.089
C–Z	1.089	1.088	1.094	1.088	1.086	1.092	1.089
C–S	1.797 (1.812)[c]	1.817	1.794	1.797	1.809	1.785	1.808
S–W	1.335	1.337	2.059	1.337	1.337	2.052	2.059
Y–C–Z	108.9	110.2	109.1	106.8	106.2	109.6	110.4
Y–C–X	107.1	107.6	110.3	109.8	111.3	107.8	108.9
X–C–Z	107.8	107.6	109.1	106.8	106.9	108.3	108.9
Y–C–S	111.3	111.0	111.2	113.5	113.2	110.4	110.4
Z–C–S	106.4	111.0	105.8	105.9	111.0	104.8	110.4
X–C–S	115.1	109.4	111.3	113.5	108.0	115.7	107.8
W–S–C	95.6	94.0	99.8	94.8	93.9	99.2	96.2
W–S–C–X	66.3	179.9	61.7	63.1	179.6	71.2	−179.9
W–S–C–Y	−55.9	−61.4	−61.7	−63.1	−55.8	−51.8	−61.3
W–S–C–Z	174.3	61.4	180.0	−179.0	63.5	169.6	61.1

a) Bond lengths are given in angstroms and angles in degrees. b) C–Cl bond length in chloromethane. c) C–S bond length in methanethiol.

As shown in Table 1, the Gibbs free energy of the *gauche* conformer **1a** was smaller than the *anti* conformer **1b** at all mentioned levels. The difference in Gibbs free energy between *gauche* and *anti* conformers at MP2/6-311+G(d,p) level dropped from 17.2 kJ mol^{-1} in fluoromethanethiol[37] to 6.1 kJ mol^{-1} in chloromethanethiol. Hence, substitution of F by Cl in CH$_2$-FSH reduces anomeric effect. ZPE correction reduced this energy in chloromethanethiol by 1.5 kJ mol^{-1}. Energy data show that the electron correlation decreases the relative Gibbs free energy from 7.8 kJ mol^{-1} (HF method) to 6.1 kJ mol^{-1} (MP2 method).

The resulting potential curve (Fig. 1) of CH$_2$ClSH at the MP2/6-311G(d,p) level of theory had minima for the *gauche* and *anti* conformers at φ(H–S–C–Cl) = 66.3 and 179.9°, respectively. In contrast to the conformational behavior of CH$_2$-FSH,[37] the *anti* structure of CH$_2$ClSH with φ(H–S–C–Cl) = 179.9° is thought to be an intermediate. The $\Delta G^{\#}$ on going from *gauche* conformer to TS1 is 10.96 kJ mol^{-1}, as shown at top of Fig. 1.

The C–S bond in the *gauche* conformer of CH$_2$ClSH was calculated to be 1.797 Å at the MP2/6-311+G(d,p) level of theory, which is shorter than the C–S bond in methanethiol, by 0.015 Å. On the other hand, the C–Cl bond of CH$_2$ClSH was calculated to be 1.785 Å at the same level of calculation, which is 0.01 Å longer than the C–Cl bond in chloromethane (see Table 2). The shortening of the C–S bond, lengthening of the C–Cl bond and increase in the S–C–Cl angle in *gauche* conformer **1a** relative to the *anti* conformer **1b** at the MP2/6-311+G(d,p) level of theory can be explained by an AE. Comparison of C–S bond length in *gauche* conformer of CH$_2$FSH (1.791 Å)[37] and CH$_2$ClSH (1.797 Å) shows that the AE de-

creases when moving to higher rows of periodic table.

The results in Table 1 indicate that the Gibbs free energy of CH$_3$SCl is 40.8 kJ mol^{-1} higher than the CH$_2$ClSH. The potential scan for the internal rotation about the C–S bond is shown in Fig. 1c. The Gibbs free energy rotational barrier was 11.9 kJ mol^{-1}, as shown at the top of curve in Fig. 1c. The C–S bond length in **1a** (1.797 Å) was greater than that in **1c** (1.794 Å).

CHCl$_2$SH (2a and 2b).   Figure 2a shows the potential scan for the internal rotation about the C–S bond for **2a** compound at the MP2/6-311G(d,p) level of theory. The resulting potential curve (Fig. 2a) of CHCl$_2$SH had minima for conformers **2a** and **2b** at φ(W–S–C–X) = 63.1 and 179.6°, respectively. The calculated Gibbs free energy difference between **2a** and **2b** conformers was 3.3 kJ mol^{-1}. The Gibbs free energy barrier in going from **2a** conformer to **TS1** is 10.7 kJ mol^{-1}, as shown at top of Fig. 2a. In the lowest energy conformation (**2a**) of CHCl$_2$SH compound, thiol hydrogen was *gauche* to the maximum number of halogens, despite the steric penalty incurred for adopting such a position. The shortening of the C–S bond by 0.012 Å, lengthening of the C–Cl(X) and C–Cl(Y) bonds, respectively, by 0.01 and 0.001 Å, and increase in the S–C–Cl(X) angle by 5.5° in conformer **2a** relative to the **2b** at the MP2/6-311+G(d,p) level of theory can also be attributed to an AE.

The barriers to rotation about the C–S bond in *gauche* conformation of CH$_2$ClSH and CHCl$_2$SH were approximately identical. For CH$_2$ClSH and CHCl$_2$SH compounds, the Gibbs free energy difference between the two possible conformers was 6.1 and 3.3 kJ mol^{-1}, respectively. Hence, energetic preference at MP2/6-311+G(d,p) level is slightly greater in CH$_2$-ClSH than in CHCl$_2$SH.
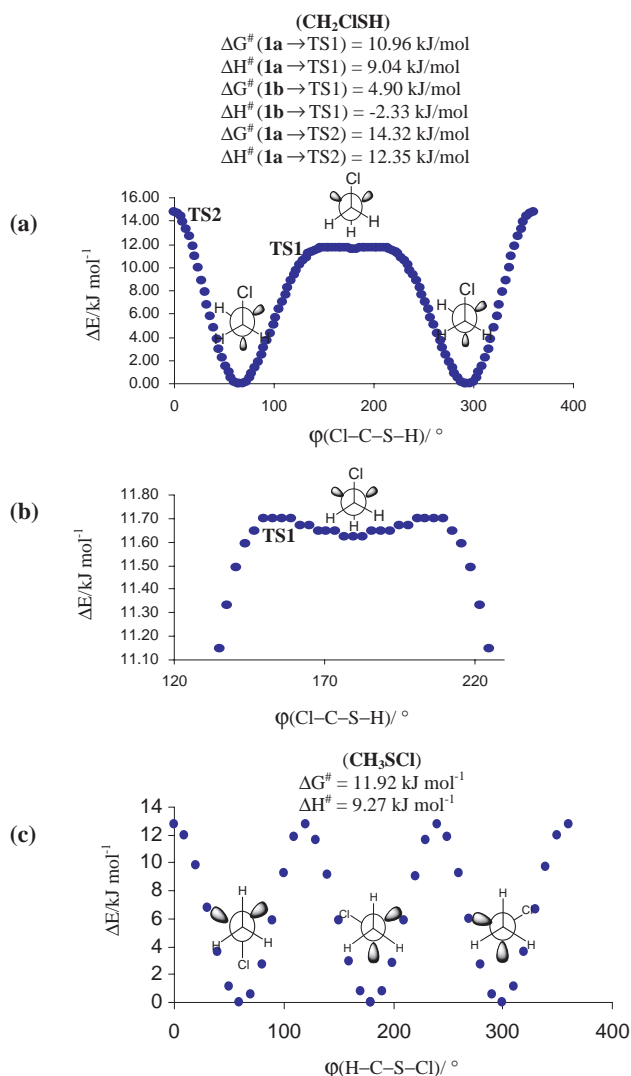
(CH₂ClSH)
$\Delta G^{\#}$ (**1a** → TS1) = 10.96 kJ/mol
$\Delta H^{\#}$ (**1a** → TS1) = 9.04 kJ/mol
$\Delta G^{\#}$ (**1b** → TS1) = 4.90 kJ/mol
$\Delta H^{\#}$ (**1b** → TS1) = -2.33 kJ/mol
$\Delta G^{\#}$ (**1a** → TS2) = 14.32 kJ/mol
$\Delta H^{\#}$ (**1a** → TS2) = 12.35 kJ/mol

(a)

(b)

(CH₃SCl)
$\Delta G^{\#}$ = 11.92 kJ mol⁻¹
$\Delta H^{\#}$ = 9.27 kJ mol⁻¹

(c)

Fig. 1. Calculated potential energy curve for rotation around the S–C bond at MP2/6-311G(d,p) level. (a) and (b) (expanded) for CH₂ClSH and (c) for CH₃SCl. Activation energies at MP2/6-311+G(d,p) level are given at top of curves.

(CHCl₂SH)
$\Delta G^{\#}$ (**2a** → TS1) = 10.69 kJ/mol
$\Delta H^{\#}$ (**2a** → TS1) = 8.59 kJ/mol
$\Delta G^{\#}$ (**2b** → TS2) = 7.37 kJ/mol
$\Delta H^{\#}$ (**2b** → TS2) = 5.11 kJ/mol

(a)

(b)

(CH₂ClSCl)
$\Delta G^{\#}$ (**2c** → TS1) = 15.82 kJ/mol
$\Delta H^{\#}$ (**2c** → TS1) = 11.68 kJ/mol
$\Delta G^{\#}$ (**2d** → TS1) = 10.07 kJ/mol
$\Delta H^{\#}$ (**2d** → TS1) = 4.59 kJ/mol

Fig. 2. Calculated potential energy curve for rotation around the S–C bond at MP2/6-311G(d,p) level. (a) For CHCl₂SH and (b) for CH₂ClSCl. Activation energies at MP2/6-311+G(d,p) level are given at the top of curves.

CH₂ClSCl (2c and 2d). The potential scan for the internal rotation about the C–S bond in compound **2c** is shown in Fig. 2b. The $\Delta G^{\#}$ on going from TS1 was 15.8 kJ mol⁻¹, as shown at the top of curve in Fig. 2b. The Gibbs free energy of the *gauche* conformer **2c** at the MP2/6-311+G(d,p) level is 5.8 kJ mol⁻¹ lower than the *anti* **2d** one, as given in Table 1. Therefore, the energetic preference of most stable conformer at MP2/6-311+G(d,p) level is slightly greater in CH₂ClSCl than in CHCl₂SH. As a result, the order of energetic preference of most stable conformers in studied compounds is CH₂ClSH > CH₂ClSCl > CHCl₂SH.

The shortening of the C–S bond by 0.023 Å, lengthening of the C–Cl bond by 0.009 Å and increase of the S–C–Cl angle by 7.9° in *gauche* conformer **2c** relative to the *anti* conformer **2d** at the MP2/6-311+G(d,p) level of theory can also be explained by anomeric effect.

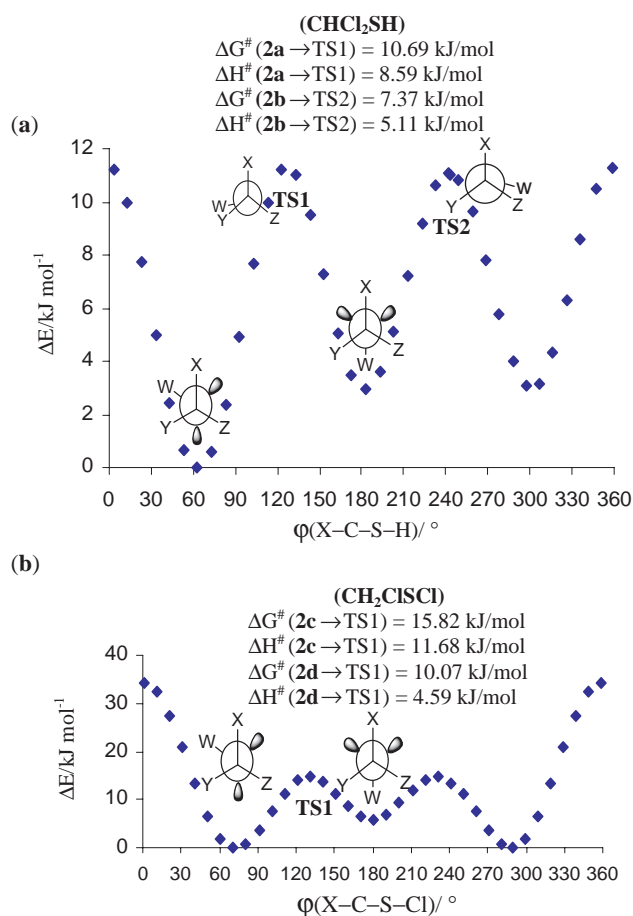**Natural Bond Orbital Analysis.** Among theoretical methods, natural bond orbital (NBO) analysis is a unique approach to the evaluation of the delocalization effects.[6,17,18,38,39] The most important interactions between donor and acceptor NBOs are reported in Table 3. In addition, occupancies of natural bonds and lone pairs, natural charges, and %p-character of sulfur atom are given in Table 4. Total energies, Lewis energies, and electronic delocalization contribution to the anomeric effect are also given in Table 5.

CH₂ClSH. From results of NBO analysis collected in Table 3, in the *gauche* structure **1a**, the charge-transfer energies of lp₂(S) → σ*(C–Cl) and lp₂(S) → σ*(C–H) interactions were 55.1 and 18.4 kJ mol⁻¹, respectively. These two interactions represent approximately 23% of the total delocalization energy (324.0 kJ mol⁻¹). In the *anti* structure **1b** the lp₂(S) participate in two lp₂(S) → σ*(C–H) interactions with total charge-transfer energy of 50.4 kJ mol⁻¹. Dependence of most important delocalization energy $E^{(2)}$ on the φ(X–C–S–H) dihedral angle is shown in Fig. 3. As can be observed, the strength of delocalization energy of lp₂(S) → σ*(C–Cl) interaction increased going from the eclipsed (φ = 0.0°) to *gauche* (φ = 66.3°) structure and then decreased. In addition, reduction of delocalization energy of lp₂(S) → σ*(C–Z(H)) interaction was accompanied by an increase in lp₂(S) → σ*(C–Y(H)) interaction on rotation. It should be noted that although delocalization energy of lp₂(S) → σ*(C–Cl) interaction at $\varphi \approx 85.0°$

Table 3. The Second-Order Perturbation Energy $E^{(2)}$ (kJ mol^{-1}) (Donor → Acceptor) Calculated at the MP2/6-311+G(d,p) Level

Donor	Acceptor	1a	1b	1c	2a	2b	2c	2d
lp$_1$(S)	σ^*(C–Y)	6.4	2.2	—	10.2	5.2	4.3	—
lp$_1$(S)	σ^*(C–Z)	3.3	2.2	—	4.2	5.7	—	—
lp$_1$(S)	σ^*(C–X)	3.0	—	—	10.2	—	2.4	—
lp$_2$(S)	σ^*(C–Y)	18.4	25.2	27.6	41.9	45.6	16.9	26.1
lp$_2$(S)	σ^*(C–Z)	—	25.2	27.6	—	25.3	—	26.1
lp$_2$(S)	σ^*(C–X)	55.1	—	—	41.9	—	59.4	—
lp$_2$(X)	σ^*(C–S)	—	—	—	29.9	25.4	17.8	15.1
lp$_3$(X)	σ^*(C–S)	35.7	31.1	13.7	29.9	21.9	36.9	30.0

Table 4. NBO Analysis Data Calculated at the HF/6-311+G(d,p) Level of Theory

	Occupancy						
	1a	1b	1c	2a	2b	2c	2d
C–Y	1.9948 (1.9952)$^{a)}$	1.9961	1.9963	1.9929	1.9936	1.9932	1.9951
C–Z	1.9920 (1.9951)	1.9961	1.9868	1.9897	1.9936	1.9857	1.9955
σ^*(C–X)	0.0385 (0.0181)	0.0141	—	0.0593	0.0421	0.0408	0.0158
C–S	1.9931 (1.9935)	1.9930	1.9933	1.9911	1.9911	1.9925	1.9904
lp$_1$(S)	1.9921 (1.9953)	1.9944	1.9954	1.9844	1.9919	1.9939	1.9963
lp$_2$(S)	1.9518 (1.9691)	1.9734	1.9690	1.9456	1.9542	1.9463	1.9700
Natural charge							
C	−0.4708 (−0.4612)	−0.4545	−0.6589	−0.3815	−0.3686	−0.5571	−0.5273
S	0.0409 (0.0290)	0.0318	0.2633	0.0846	0.0811	0.2913	0.2741
X	−0.0677 (−0.0486)	−0.0481	−0.2051	−0.0101	0.0022	−0.0177	0.0022
% p-Character of sulfur							
C–S	82.1 (83.2)	83.1	81.0	82.6	83.3	81.7	82.8
lp$_1$	33.8 (30.4)	29.7	24.8	30.4	31.6	26.4	22.8
lp$_2$	97.2 (99.6)	100.0	100.0	100.0	97.9	97.9	100.0

a) NBO data for TS1 is given in the parentheses.

Table 5. Total Energy, Lewis Energy (in au), and Electronic Delocalization Contribution to the AE ($\Delta\Delta E_{del}$ in kJ mol^{-1}) Calculated at the HF/6-311+G(d,p) Level of Theory

	1a	1b	1c	2a	2b	2c	2d
E_{tot}	−896.66227	−896.65874	−896.65359	−1355.57493	−1355.57415	−1355.57178	−1355.57079
E_{Lewis}	−896.53876	−896.54604	−896.56850	−1355.36977	−1355.37414	−1355.42148	−1355.43472
ΔE_{del}	−324.0	−295.6	−223.2	−538.1	−524.3	−394.3	−356.9
ΔE_{total}	0.0	9.3	22.8	0.0	2.3	0.0	2.6
ΔE_{Lewis}	0.0	−19.1	−78.0	0.0	−11.4	0.0	−34.7
$\Delta\Delta E_{del}{}^{a)}$	0.0	28.4	100.8	0.0	13.8	0.0	37.4

a) $\Delta\Delta E_{del} = (E_{total} - E_{Lewis})_{anti} - (E_{total} - E_{Lewis})_{gauche}$.

(Fig. 3a) is a maximum, the most stable conformer (*gauche*) is formed at $\varphi = 66.3°$ (Table 2). Therefore, the most stable conformation of CH$_2$ClSH may also be influenced by some other factors, such as weak interactions.

Because of stronger hyperconjugative interactions with σ^*(C–Cl) in **1a** with respect to the **1b**, σ^*(C–Cl) occupation number in **1a** was greater than **1b** by 0.0244e. In **1a**, the lp$_2$(S) → σ^*(C–Cl) interaction is stronger than lp$_3$(Cl) → σ^*(C–S) interaction (with 35.7 kJ mol^{-1} energy), and in the **1b**, the lp$_3$(Cl) → σ^*(C–S) interaction (with 31.1 kJ mol^{-1} energy) was weaker than two lp$_2$(S) → σ^*(C–H) interactions with the total charge-transfer energy of 50.4 kJ mol^{-1}. The

lp$_3$(Cl) → σ^*(C–S) interaction energy in both conformers is almost identical.

The changes in charge-transfer energies of lp$_2$S → σ^*(C–X) (X = F and Cl) on rotation in CH$_2$XSH are compared in Fig. 3a. From comparison of charge-transfer energies of lp$_2$S → σ^*(C–X) (X = F and Cl) and of lp$_2$S → σ^*(C–Y(H)) interactions in *gauche* conformer of CH$_2$FSH[37] and CH$_2$ClSH (see Table 3), it can be seen that when moving down through the group 17 of periodic table the charge-transfer energy of lp$_2$S → σ^*(C–X) interaction decreases from 69.4 to 55.1 kJ mol^{-1} and that of lp$_2$S → σ^*(C–Y) interaction increases from 13.1 to 18.4 kJ mol^{-1}. The differences in the
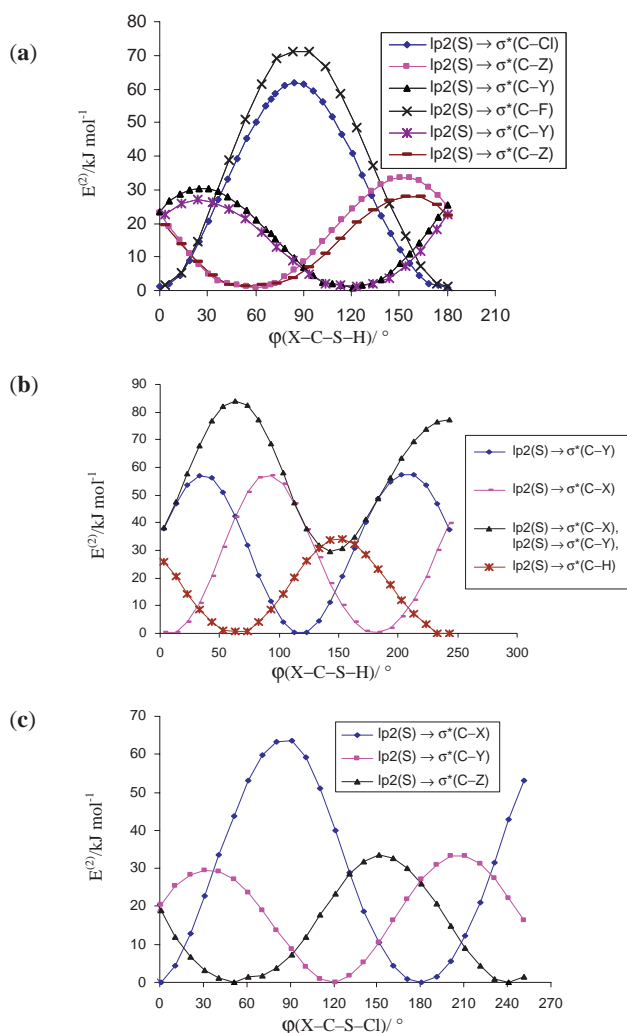
Fig. 3.   Dependence of $E^{(2)}$ on the $\varphi(\text{X–C–S–H})$ dihedral angle. (a) CH_2ClSH and CH_2FSH, (b) $CHCl_2SH$, and (c) CH_2ClSCl.

trends involving the $\sigma^*(\text{C–F})$ and $\sigma^*(\text{C–Cl})$ antibonds as acceptors can be rationalized quantitavely through NBO analysis of $E^{(2)}$. For each donor NBO (i) and acceptor NBO (j), $E^{(2)}$ associated with delocalization i → j was estimated as $E^{(2)} = \Delta E_{ij} = -q_j F(i,j)^2/(\varepsilon_i - \varepsilon_j)$, where q_i is the donor orbital occupancy, ε_i, ε_j are diagonal elements (orbital energies) and $F(i,j)$ is the off-diagonal NBO Fock matrix element. NBO calculations showed that the values of $\Delta\varepsilon$ and $F(i,j)$ included in $E^{(2)}$ term decrease, respectively, from 0.85 and 0.106 au in $lp_2S \rightarrow \sigma^*(\text{C–F})$ interaction to 0.71 and 0.087 au in $lp_2S \rightarrow \sigma^*(\text{C–Cl})$ one. Therefore, trends in the donor ability of the sulfur lone pair toward $\sigma^*(\text{C–X})$ orbitals are controlled by increasing the $F(i,j)$ term by 0.019 au on going from Cl to F. The increase in energy of $lp_2S \rightarrow \sigma^*(\text{C–Y})$ interaction in going from CH_2FSH to CH_2ClSH can be attributed to increasing of $F(i,j)$ term by 0.01 au.

From Table 4, the lone pairs of sulfur atom are directionally inequivalent in the *gauche* structure: one occupies an orbital with considerable p-character (97.2%) and a low occupation number (1.9518e) and the other occupies an orbital with p-character (33.8%) and high occupation number (1.9921e).

The p-character of the sulfur lone pair, in which participate in lp(S) → $\sigma^*(\text{C–Cl})$ interaction in the *gauche* ($lp_2(S)$) and *anti* ($lp_1(S)$) structures were 97.2 and 29.7%, respectively. The obtained results show that donor ability decreases with an increase in the s-character of a lone pair and lone pairs with 100% p-character are intrinsically better donors than respective sp^n hybrid orbitals.

The natural charge distribution of **1a** (*gauche* structure) calculated at the HF/6-311+G(d,p) level (Table 4) shows that both the C and Cl carry negative charges of −0.4708e and −0.0677e, respectively, and S carries a positive charge of 0.0409e. For the *anti* structure **1b**, the negative charge on the Cl (−0.0481e) was smaller than corresponding atom in the *gauche* structure by 0.0196e. Therefore, lp(S) → $\sigma^*(\text{C–Cl})$ interaction in the *gauche* structure is stronger than *anti* structure, causing a large negative charge on the Cl atom in the *gauche* structure.

Studies on the compounds involving atoms with different types of lone pairs show that the effect of charge delocalization should not be studied comparing only lp → σ^* interactions, since $\sigma \rightarrow \sigma^*$ interactions and interactions involving Rydberg orbitals can have relative importance.[9,12] Thus, NBO analysis at the HF/6-311+G(d,p)//MP2/6-311+G(d,p) level was also carried out using NOSTAR keyword for zeroing all orbital interactions (off-diagonal Fock matrix elements). As it can be seen from Table 5, the difference between total and Lewis energies ($\Delta E_{del} = E_{total} - E_{Lewis}$) as a measure of loss of stabilization for the *gauche* structure **1a** was −324.0 kJ mol^{-1} (equal to 0.014% of the total energy). ΔE_{del} for the *anti* structure **1b** was −295.6 kJ mol^{-1} (equal to 0.012% of the total energy), implying a smaller amount of charge delocalization in the *anti* structure than *gauche* one. The Lewis energy difference (ΔE_{Lewis}) is a measure of molecular stability in the absence of stereoelectronic interactions. In the absence of electronic delocalization, steric effects would be dominant in *gauche* conformer (with greater Lewis energy than *anti*) and a preference for the *anti* conformer would predominate.

The relative total energies of the various conformers as well as the Lewis and delocalization energy contributions to the relative energies upon rotation for CH_2ClSH and CH_2FSH are presented in Fig. 4a. From Fig. 4a, it is evident that in going from *gauche* conformer to *anti* one, difference between ΔE_{tot} and $\Delta\Delta E_{del}$ increases, indicating charge delocalization contributions to the total energy decreases. Amount of this difference for CH_2ClSH was firstly greater than CH_2FSH on going from *gauche* to anti, but it inverted for $\varphi > 130°$. For $\varphi \lesssim 70.0°$, a larger decrease in the charge delocalization contributions to the total energy for CH_2FSH is mainly due to greater increase of Lewis contribution in CH_2FSH with respect to CH_2ClSH. On the other hand, as the Lewis contribution increases on going from *gauche* to *anti*, contribution of delocalization on total energy decreases. Similarity between the total energy change and delocalization energy change reveals the influence that the Lewis contribution has on reducing the rotational barrier. Decrease in rotational barrier on going from CH_2FSH to CH_2ClSH is expected due to an increase in the Lewis contribution and a decrease in delocalization. Besides, Figure 4a shows that the variations of delocalization contribution in both compounds are greater than varia-
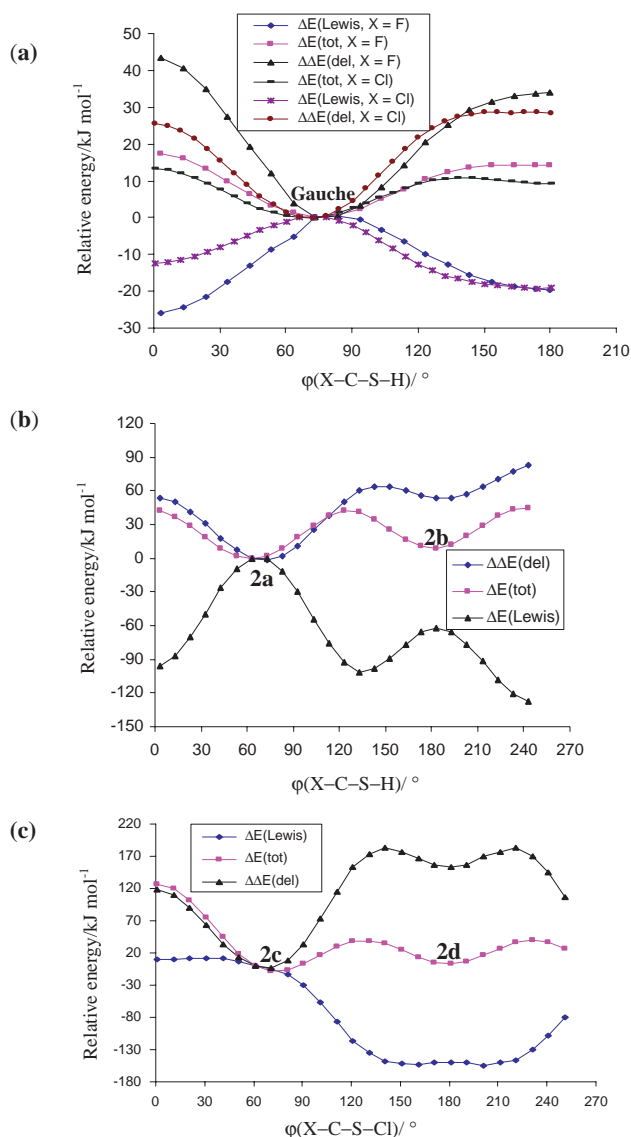
(a)

(b)

(c)

Fig. 4.   Variation in E_{tot}, E_{Lewis}, and E_{del} with a change in $\varphi(X–C–S–H(Cl))$ dihedral angle. (a) CH$_2$ClSH and CH$_2$-FSH, (b) CHCl$_2$SH, and (c) CH$_2$ClSCl.

tions of Lewis energy contribution for all dihedral angles. Therefore, the electrostatic and steric contributions included in the Lewis term are less important than delocalization contribution to rotation.

The structural effects of electron delocalization can be examined by coupling the NBO energetic analysis to numerical geometry optimization using the Gaussian program package. The hyperconjugative delocalizations effects on the structural parameters obtained by HF/6-311+G(d,p) method are given in Table 6. As can be seen from this Table, in the absence of the lp(S) → σ*(C–Cl) interaction, the geometry distortion in the *gauche* conformer was greater than in *anti* one.

The rotational energy barrier can be decomposed into structural (bond and lone pair energy), steric repulsion and delocalization energy changes ($\Delta E_{barrier} = \Delta E_{struct} + \Delta E_{deloc} + \Delta E_{steric}$).[40,41] The individual energy contributions ($\Delta\omega$) forming structural energy and sum of bond and lone pair energy change ($\sum \Delta\omega$) are listed in Table 7. As given in this Table,

Table 6.   Hyperconjugative Delocalizations Effects on the Structural Parameters: (**d**) Deletion of lp(S) → σ*(C–Cl) and lp(S) → σ*(C–H) Hyperconjugative Interactions; (**f**) Deletion of lp(S) → σ*(C–Cl) Hyperconjugative Interaction

Parameter	d		f	
	1a	**1b**	**1a**	**1b**
Δ(C1–Cl)[a)]	0.011	−0.044	0.039	−0.007
Δ(C1–H)	−0.009	0.011	0.014	0.012
Δ(C1–S)	−0.068	−0.032	−0.054	0.000
Δ(Cl–C–S)[b)]	7.8	4.1	4.0	0.1
Δ(W–S–C)	−2.9	−5.0	−1.9	−1.5
Δ(W–S–C–Cl)[b)]	96.1	−17.3	−66.0	0.0

a) Bond lengths are in angstroms. b) Angles are in degrees.

Table 7.   HF/6-311+G(d,p) Calculated Change in Bond and Lone Pair Energies on Rotation

	$\Delta\omega$[a)](GS → TS1)		
	1a	**2a**	**2c**
C–S	97.9	101.9	0.7
lp$_1$S	−95.5	64.6	44.6
lp$_2$S	58.6	−47.9	7.6
C–X	−34.5	8.3	−10.9
C–Y	−12.2	−62.6	49.3
C–Z	−19.1	−9.1	−4.4
S–W	14.5	−37.3	11.2
lp$_1$X	−70.0	39.8	19.0
lp$_2$X	−11.6	−21.1	−20.7
lp$_3$X	53.5	18.1	−19.2
lp$_1$Y	—	−54.1	62.6
lp$_2$Y	—	−37.4	22.2
lp$_3$Y	—	−25.8	−1.1
$\sum \Delta\omega$[b)]	−18.5	−62.4	161.0

a) $\Delta\omega = \varepsilon_t N_t - \varepsilon_e N_e$.[38,40,41] b) Structural energy in kJ mol^{-1}.

the changes of lp$_1$(S), lp$_2$(S), and C–S NBOs energies on rotation in **1a** were −95.5, 58.6, and 97.9 kJ mol^{-1}, respectively. Hence the lp$_2$(S) and C–S NBOs are the most important barrier forming energy contributions. The NBOs energy is sensitive to changes in hybridization. In other words, the significant source of the NBO energy increase is the 1.1 and 2.4% increase in p-character of sulfur of C–S and lp$_2$(S) in TS1 (Table 4 and Fig. 1a), respectively. The barrier forming structural energy change on rotation in **1a** is (−18.5 kJ mol^{-1}) anti-barrier (i.e., negative).

The AE in CH$_3$SCl is expected to be weaker than CH$_2$ClSH. The sum of $E^{(2)}$ terms corresponding to interactions of the S lone pairs (lp$_1$ and lp$_2$) with σ*(C–H) antibond in **1c** compound was 55.2 kJ mol^{-1}. It is noteworthy from the NBO data in Table 3 that the **1a** structure benefits from one strong lp(S) → σ*(C–Cl) interaction with 55.1 kJ mol^{-1} energy, while this interaction is absent in **1c**. The natural charges in Table 4 indicate that the positive charge on the S (0.2633e) in **1c** structure is larger than that in **1a** structure by 0.2224e.

CHCl$_2$SH (2a and 2b).   Influence of rotation about the C–S bond on the most important interaction energies is shown in Fig. 3b. As can be seen from Fig. 3b, the strength of delocalization energy of lp$_2$(S) → σ*(C–X) and lp$_2$(S) → σ*(C–Y)

interactions between dihedral angle φ(H–S–C–X) 0 and 63.0° was different, but in 63.0° (**2a**) were equal. In conformation **2b** ($\varphi = 180.0°$), the delocalization energy of $lp_2(S) \to \sigma^*(C–X)$ interaction was nearly zero, whereas its value for $lp_2(S) \to \sigma^*(C–Y)$ interaction was 41.9 kJ mol^{-1}. In other words, NBO results (Table 3 and Fig. 3b) show that conformer **2a** benefits from two strong $lp_2(S) \to \sigma^*(C–Cl)$ interactions each with a delocalization energy of 41.9 kJ mol^{-1}, whereas the conformer **2b** has one such interaction with 45.6 kJ mol^{-1}. Owing to the presence of two $lp_2(S) \to \sigma^*(C–Cl)$ donor–acceptor interactions in **2a**, the stability of **2a** structure is greater than **2b** one.

In contrast with the CH$_2$ClSH, the calculated natural charge distribution of **2a** and **2b** indicates (Table 4) that the both Cl carry partially positive charges. The NBO analysis also describes the bonding in terms of the natural hybrid orbitals. From Table 4, in conformers **2a** and **2b**, one of the lone pairs (lp2) of sulfur atom had considerable p-character (100.0% for **2a** and 97.9% for **2b**) and the other have ≈30.0% p-character. Hence, a nearly pure p-type lone pair orbital participates in the electron donation to the $\sigma^*(C–Y(Cl))$ orbital $[lp_2S \to \sigma^*(C–Cl)]$ in conformers **2a** and **2b**.

For the **2a** ⇌ **2b** equilibrium, Lewis energy difference was negative (-11.4 kJ mol^{-1}) and $\Delta\Delta E_{deloc}$ was positive (13.8 kJ mol^{-1}) (Table 5), indicating conformer **2a** is favored when electronic delocalization is dominant and **2b** is preferred when steric effects predominate. The relative total energies of the various conformers as well as the Lewis and delocalization energy contributions to the relative energies upon rotation for CHCl$_2$SH are presented in Fig. 4b. From Fig. 4b, it is evident that on going from conformer **2a** to **2b** one, the difference between ΔE_{tot} and $\Delta\Delta E_{del}$ increases, indicating charge delocalization contributions to the total energy decrease and Lewis contributions increase.

The change in $lp_1(S)$, $lp_2(S)$, and C–S NBO energies on rotation in **2a** was 64.6, -47.9, and 101.9 kJ mol^{-1}, respectively, as given in Table 7. Hence, the $lp_1(S)$ and C–S NBOs are the most important barrier forming energy contribution. The significant source of the NBO energy increase in **2a** is the 0.7 and 1.5% increase in p-character of sulfur atom in C–S bond and $lp_1(S)$ NHOs of the top-of-barrier of **2a**, respectively. The structural energy on rotation in **2a** was -62.4 kJ mol^{-1}. Hence, structural energy term of rotational barrier in **2a** is anti-barrier.

CH$_2$ClSCl (2c and 2d).   Correlations of φ(Cl–S–C–Cl) dihedral angle with the energy of the most important interaction energies are shown in Fig. 3c. The strength of delocalization energy of $lp_2(S) \to \sigma^*(C–Cl)$ interaction increased on going from the eclipsed structure ($\varphi = 0.0°$) to *gauche* ($\varphi = 73.1°$) one, then decreased, and finally become zero in for the *anti* conformation ($\varphi = 180.0°$). In *anti* conformation the $lp_2(S) \to \sigma^*(C–Cl)$ interaction was replaced by two $lp_2(S) \to \sigma^*(C–H)$ interactions. In addition, reduction of delocalization energy of $lp_2(S) \to \sigma^*(C–Z(H))$ interaction was accompanied by an increase in the $lp_2(S) \to \sigma^*(C–Y(H))$ interaction on rotation. Hence, the NBO results (Table 3 and Figure 3c) show that in the *gauche* conformer **2c**, $lp_2(S)$ participates in $lp_2(S) \to \sigma^*(C–Cl)$ interaction with a charge-transfer energy of 59.4 kJ mol^{-1}, while the strength of this interaction in **2d** is smaller than threshold limit (2.1 kJ mol^{-1}). Since $lp_2(S) \to$

$\sigma^*(C–Cl)$ orbital interaction is nearly absent in conformer **2d**, stabilization of conformer **2c** vs. **2d** results. Because of the different charge-transfer interactions, the occupation number of $\sigma^*(C–Cl)$ in **2c** (0.0408e) is greater than **2d** (0.0158e). The relative total energies of the various conformers as well as the Lewis and delocalization energy contributions to the relative energies upon rotation for CH$_2$ClSCl are presented in Fig. 4c. The Lewis energy term was small and positive for dihedral angles between 0.0 and 73.1° and then increased on going from *gauche* conformer to *anti* one, as shown in Fig. 4c. the decrease in the charge delocalization contributions to the total energy is mainly due to increases of Lewis contributions in going from *gauche* conformer to *anti* one.

For the **2c** ⇌ **2d** equilibrium, Lewis energy difference was negative (-34.7 kJ mol^{-1}), and $\Delta\Delta E_{deloc}$ was positive (37.3 kJ mol^{-1}), indicating that conformer **2c** is favored when electronic delocalization is dominant and **2d** is preferred when the steric effects predominate. On the other hand, the absolute value of ΔE_{Lewis} and $\Delta\Delta E_{deloc}$ in CH$_2$ClSCl was greater than CHCl$_2$SH. Therefore, it is expected that the energetic preference of most stable conformer in CH$_2$ClSCl is greater than that of CHCl$_2$SH.

As shown in Table 7, the change of $lp_1(S)$, $lp_2(S)$, and C–S NBOs energy on rotation in **2c** was 44.6, 7.6, and 0.7 kJ mol^{-1}, respectively. Hence energy of $lp_1(S)$ is the dominant term in structural energy. The change in the percentage of p-character in $lp_1(S)$, $lp_2(S)$, and sulfur atom of C–S bond on rotation was -2.8, 1.9, and 1.0, respectively. The structural energy on rotation in **2c** was 161.0 kJ mol^{-1}. Hence, it is expected that the structural energy term contributes to the rotational energy barrier of **2c**.

Computational Details

Potential scans for the internal rotation about the C–S bond were performed by using geometry optimization at fixed dihedral angles φ(W–S–C–X) of 0–360° with MP2/6-311G(d,p) method. All of the structures studied in this work were fully optimized at the HF/6-311+G(d,p), B3LYP/6-311+G(d,p), and MP2/6-311+G(d,p) levels of theory. The vibrational frequencies were also calculated at the same levels to characterize the stationary points and calculation of thermal corrections. All computations were performed using the Gaussian-98 program package.[42] The NBO analysis[43] was carried out on the HF/6-311+G(d,p) wave functions obtained from the MP2/6-311+G(d,p) optimized geometries using version 3.1 of NBO package[44] included in Gaussian-98 program.

Conclusion

The data and discussion in previous sections, lead us to the following major conclusions. The *gauche* conformers, that is, **1a**, **2a**, and **2c** were predicted to be more stable than corresponding *anti* ones. The order of energetic preference of most stable conformers in studied compounds was CH$_2$ClSH > CH$_2$ClSCl > CHCl$_2$SH. Also, substitution of F by Cl in CH$_2$-FSH reduced the AE. NBO analysis at the HF/6-311+G(d,p) level indicates that the conformational preference of **1a**, **2a**, and **2c** conformers over **1b**, **2b**, and **2d** ones, respectively is the result of a wide variety of orbital interactions. However, interactions between the lp(S) and the $\sigma^*(C–Cl)$ are the most

important factors for stabilizing the *gauche* conformers. The strength of delocalization energy of $lp_2(S) \rightarrow \sigma^*(C-Cl)$ interaction in all compounds increased on going from the eclipsed ($\varphi = 0.0°$) to *gauche* structure and then decreased. From comparison of charge-transfer energy of $lp_2S \rightarrow \sigma^*(C-X)$ (X = F and Cl) interaction in *gauche* conformer of CH_2FSH and CH_2ClSH, it can be seen that when moving down through the group 17 of periodic table the charge-transfer energy of $lp_2S \rightarrow \sigma^*(C-X)$ interaction decreases. In the absence of the $lp(S) \rightarrow \sigma^*(C-Cl)$ hyperconjugative interaction in **1a**, the geometry distortion in the *gauche* conformer is greater than the *anti* one. Difference between total and Lewis energies for the *gauche* structure of **1a**, **2a**, and **2c** is greater than corresponding *anti* structures (**1b**, **2b**, and **2d**), which imply a lower charge delocalization in the *anti* structures than *gauche* ones. From the $\Delta\Delta E_{del}$ values, it can be concluded effect of hyperconjugative stabilization is always stronger than effect of energy of the conformers considered as hypothetical Lewis structures. Hence, the electrostatic and steric contributions involved in the Lewis term are less important than the charge delocalization. In addition, for all compounds, the difference between ΔE_{tot} and $\Delta\Delta E_{del}$ on going from *gauche* conformer to *anti* one increase, indicating charge delocalization contributions to the total energy decreases and Lewis contributions increases. The structural energy on rotation in **1a**, **2a**, and **2c** was -18.5, -62.5, and $161.0 \, kJ \, mol^{-1}$, respectively. Hence, the structural energy term of rotational barrier in **1a** and **2a** is anti-barrier.

References

1   T. Laube, T.-K. Ha, *J. Am. Chem. Soc.* **1988**, *110*, 5511.

2   H. D. Thomas, K. Chen, N. L. Allinger, *J. Am. Chem. Soc.* **1994**, *116*, 5887.

3   F. Bohlman, *Angew. Chem.* **1957**, *69*, 547.

4   S. Wolfe, C.-K. Kim, *Can. J. Chem.* **1991**, *69*, 1408.

5   C. Romers, C. Altona, H. R. Bouys, E. Havinga, *Topics in Stereochemistry*, **1969**, Vol. 4, p. 39.

6   P. P. Graczyk, M. Mikołajczyk, *Topics in Stereochemistry*, **1994**, Vol. 21, p. 159.

7   A. J. Kirby, *The Anomeric Effect and Related Steroelectronic Effects at Oxygen*, Springer-Verlag, Berlin, **1983**.

8   E. L. Eliel, S. H. Wilen, L. N. Mander, *Stereochemistry of Organic Compounds*, Wiley & Sons, New York, **1994**.

9   U. Salzner, P. v. R. Schleyer, *J. Am. Chem. Soc.* **1993**, *115*, 10231.

10   E. Juaristi, G. Cuevas, *The Anomeric Effect*, CRC Press, Boca Raton, FL, **1995**.

11   W. F. Schneider, B. I. Nance, T. J. Wallington, *J. Am. Chem. Soc.* **1995**, *117*, 478.

12   L. Carballeira, I. Pérez-Juste, *J. Phys. Chem. A* **2000**, *104*, 9362.

13   G. Leroy, J. P. Dewispelaere, H. Benkadour, D. R. Temsamani, C. Wilante, *THEOCHEM* **1995**, *334*, 137.

14   J. A. Pople, L. Radom, W. J. Hrhre, *J. Am. Chem. Soc.* **1971**, *93*, 289.

15   L. Radom, W. J. Hrhre, J. A. Pople, *J. Am. Chem. Soc.* **1972**, *94*, 2371.

16   S. Wolfe, A. Rauk, L. M. Tel, I. G. Csizmadia, *J. Chem. Soc. B* **1971**, 136.

17   F. Grein, P. DEslongchamps, *Can. J. Chem.* **1992**, *70*, 604.

18   F. Grein, P. DEslongchamps, *Can. J. Chem.* **1992**, *70*, 1562.

19   P. v. R. Schleyer, A. J. Kos, *Tetrahedron* **1983**, *39*, 1141.

20   G. F. Smits, M. C. Krool, C. Altona, *Mol. Phys.* **1988**, *65*, 513.

21   B. M. Pinto, H. B. Schlegel, S. Wolfe, *Can. J. Chem.* **1987**, *65*, 1658.

22   J. O. Williams, J. N. Scarsdal, L. Schäfer, *J. Mol. Struct.* **1981**, *76*, 11.

23   U. Salzner, P. v. R. Schleyer, *J. Org. Chem.* **1994**, *59*, 2138.

24   R. Kühn, D. Christen, H. G. Mack, D. Konikowski, R. Minkwitz, H. Oberhammer, *THEOCHEM* **1996**, *376*, 217.

25   S. Sakurai, N. Meinander, K. Morris, J. Laane, *J. Am. Chem. Soc.* **1999**, *12*, 5056.

26   Y. P. Chang, T. M. Su, *THEOCHEM* **1996**, *365*, 183.

27   E. E. Astrup, *Acta Chem. Scand.* **1973**, *27*, 3271.

28   K. B. Wiberg, M. A. Murcko, *J. Am. Chem. Soc.* **1989**, *111*, 4821.

29   E. E. Astrup, A. M. Aomar, *Acta Chem. Scand., Ser. A* **1975**, *29*, 794.

30   G. A. Jeffrey, J. H. Yates, *J. Am. Chem. Soc.* **1979**, *101*, 820.

31   J. R. Durig, J. Lin, G. A. Guirgis, B. J. van der Veken, *Struct. Chem.* **1993**, *4*, 103.

32   J. Nakagawa, H. Kato, M. Hayashi, *J. Mol. Spectrosc.* **1981**, *90*, 467.

33   K. I. Gobbato, H. G. Mack, H. Oberhammer, C. O. Della Vedova, *J. Am. Chem. Soc.* **1997**, *119*, 803.

34   K. Omoto, K. Marusaki, H. Hirao, M. Imade, H. Fujimoto, *J. Phys. Chem. A* **2000**, *104*, 6499.

35   D. Christen, H. G. Mack, S. Rudiger, H. Oberhammer, *J. Am. Chem. Soc.* **1996**, *118*, 3720.

36   H. Roohi, A. Ebrahimi, *THEOCHEM* **2005**, *726*, 141.

37   H. Roohi, A. Ebrahimi, S. M. Habibi, E. Jerahi, *THEOCHEM* **2006**, *772*, 65.

38   L. Goodman, V. Pophristic, *Rotational Barrier Origins*, in *Encyclopedia of Computational Chemistry*, ed. by P. v. R. Schleyer, Wiley, New York, **1998**, Vol. 4, p. 2532.

39   H. Roohi, A. Ebrahimi, F. Alirezapoor, M. Hajealirezahi, *Chem. Phys. Lett.* **2005**, *409*, 212.

40   L. Goodman, H. Gu, V. Pophristic, *J. Chem. Phys.* **1999**, *110*, 4268.

41   J. K. Badenhoop, F. Weinhold, *Int. J. Quantum Chem.* **1999**, *72*, 269.

42   M. J. Frisch, et al., Gaussian 98, Revision A.7, Gaussian, Inc., Pittsburgh PA, **1998**.

43   A. E. Reed, L. A. Curtiss, F. Weinhold, *Chem. Rev.* **1988**, *88*, 899.

44   D. E. Glendening, A. E. Reed, J. E. Carpenter, F. Weinhold, NBO, Version 3.1.